

Influence of interfacial disorder and temperature on magnetization reversal in exchange-coupled bilayers

M. R. Fitzsimmons,¹ C. Leighton,^{2,*} A. Hoffmann,¹ P. C. Yashar,¹ J. Nogués,³ K. Liu,² C. F. Majkrzak,⁴ J. A. Dura,⁴ H. Fritzsche,⁵ and Ivan K. Schuller²

¹*Los Alamos National Laboratory, Los Alamos, New Mexico 87545*

²*Department of Physics, University of California—San Diego, La Jolla, California 92093-0319*

³*Departament de Física, Universitat Autònoma de Barcelona, 08193 Bellaterra, Spain*

⁴*National Institute of Standards and Technology, Gaithersburg, Maryland 20899*

⁵*Hahn-Meitner Institut, Berlin, Germany*

(Received 14 February 2001; revised manuscript received 24 April 2001; published 22 August 2001)

Polarized neutron reflectometry is used to measure the thermal response of the net-magnetization vector of polycrystalline ferromagnetic (F) Fe films exchange coupled to twinned (110) MnF₂ antiferromagnetic (AF) layers. We observe a strong correlation between the temperature dependencies of the net sample magnetization perpendicular to the applied field at coercivity and exchange bias. For cooling field and measurement conditions involving magnetization reversal via rotation, we find a range of temperature dependencies. For the smoothest F-AF interface, the temperature dependence of exchange bias compares well to a $S = \frac{5}{2}$ Brillouin function—an observation predicted by some theoretical models. This temperature dependence is expected for the sublattice magnetization and the square root of the anisotropy constant $\sqrt{K_1}$ of bulk MnF₂. In contrast, for a rough F-AF interface the magnetization reversal process (and exchange bias) showed little temperature dependence up to temperatures approaching the AF Néel point—a clear consequence of increasing interfacial disorder in a F-AF epitaxial system.

DOI: 10.1103/PhysRevB.64.104415

PACS number(s): 75.70.Ak, 61.12.-q, 75.30.Gw

Exchange anisotropy (EA) at the interface between ferromagnetic (F) and antiferromagnetic (AF) materials is a long-standing problem in condensed-matter physics,¹ one that has received renewed attention recently due to the importance of EA in technological applications.² Progress, theoretical and experimental, has been made in understanding the phenomenology and mechanisms for exchange bias H_E (the shift of the F hysteresis loop along the field axis—a manifestation of unidirectional EA).³ Experimentally, the effects of interface disorder⁴ on H_E , the relation between H_E and coercivity, H_C ,⁵⁻⁷ the magnetization reversal mechanisms,^{8,9} and the temperature dependence of H_E (Refs. 6, 10, and 11) have been studied in different systems. Theoretical studies have produced various models for H_E and H_C .¹² These models include formation of AF domain walls parallel¹³ and perpendicular¹⁴ to the F-AF interface, perpendicular exchange coupling,¹⁵⁻¹⁷ collective excitations,¹⁸ and uncompensated free-spin densities.^{10,19} We report results of an experimental investigation that correlates temperature dependencies of magnetization reversal mechanisms and H_E with interface disorder in an epitaxial F-AF system.

Previously, polarized neutron reflectometry (PNR) was used to probe the in-plane projection of the net-magnetization vector of polycrystalline Fe films exchange coupled to twinned (110) MnF₂ or FeF₂ AF layers.⁸ For samples cooled in fields applied along a direction that bisects the anisotropy axes of the AF twins, two different magnetization reversal processes were observed. When reversing the field direction from positive to negative saturation, i.e., changing field strength from right to left along the F hysteresis loop (Fig. 1), the magnetization reversal occurred via magnetization rotation. On the other hand, when the field

was increased along the lower branch, domain nucleation (with magnetization parallel to the cooling field direction) was observed. This means that the magnetization reversal process was different on either side of the same hysteresis loop.

Here, we study the temperature dependence of the magnetization rotation process occurring at coercivity of Fe films exchange coupled to MnF₂. Using PNR, we measured the fraction of the sample with magnetization directed perpendicular to the applied field at coercivity as the sample was warmed from low temperatures to above the Néel point for

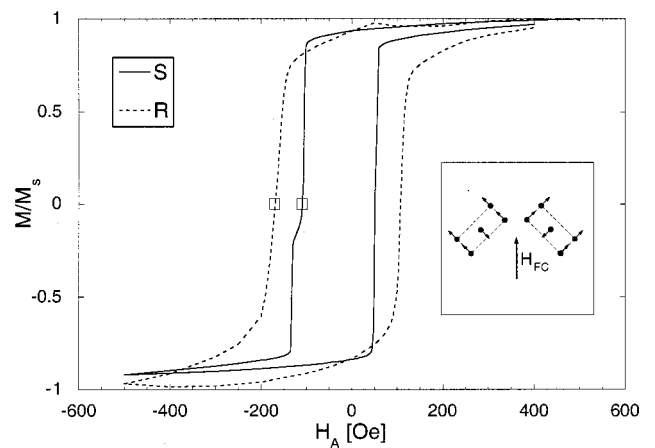


FIG. 1. Ferromagnetic hysteresis loops for samples S (solid line) and R (dashed line) at 30 K. Inset: Orientation of the 2-kOe strong cooling field relative to the MnF₂ twin domains. Arrows indicate the bulk spin structure of the AF. Neutron measurements were taken as a function of temperature for applied fields at coercivity (□).

MnF_2 ($T_N=67$ K). The neutron experiments involved studies of two samples—one with a very smooth F-AF interface and another with a more structurally disordered (rough or interdiffused) interface. We find for the case of a *smooth* F-AF interface, the fraction of the sample with magnetization directed perpendicular to the applied field at coercivity to be well correlated with H_E , and both decreased²⁰ monotonically with increasing temperature. For a *rough* F-AF interface, the magnetization reversal process was also well correlated with H_E , but a completely different thermal response compared to that of the smooth sample was observed. Neither the magnetization reversal process for the rough sample nor H_E showed appreciable temperature dependence until the temperature was within ~ 10 K of T_N , and then, the fraction of the net sample magnetization perpendicular to the applied field at coercivity (and H_E) dropped precipitously. We show that the drop of H_E near T_N is correlated with interfacial roughness for many Fe- MnF_2 samples. We attribute the dramatic difference between the thermal response of the F overlayers to the influence of F-AF interfacial disorder on the exchange coupling. In turn this quantity dictates H_E of the F hysteresis loop.

Our samples [samples for neutron study, denoted samples R (rough) and S (smooth)] were prepared by electron-beam evaporation onto single-crystal (001) MgO substrates. The samples were composed of ZnF_2 (25 nm) (buffer layers to improve epitaxy), MnF_2 (50 nm), Fe (11 nm), and Al (3 nm) (capping layer to prevent oxidation).²¹ The nominal deposition temperatures were ZnF_2 (473 ± 2 K), Fe (423 ± 2 K), and Al (423 ± 2 K). The deposition temperature of MnF_2 was varied between 523–623 K to induce different interface roughness.²¹ Using x-ray reflectometry,²² the thicknesses of the Fe films were determined to be 10 and 13 nm for samples R and S, respectively, and the roughness of the F-AF (Fe- MnF_2) interface (root-mean-square deviation about its mean) to be 1.9 ± 0.2 nm for sample R and 0.5 ± 0.2 nm for sample S.²³ In-plane glancing incidence x-ray diffraction²⁴ and reflection high-energy electron diffraction confirmed that the AF layers grew as twinned epitaxial thin films. One AF crystal domain is oriented such that $[1\bar{1}0] \text{MnF}_2 \parallel [110] \text{MgO}$, while the other domain is oriented with $[001] \text{MnF}_2 \parallel [110] \text{MgO}$. Application of the Scherrer particle size broadening relation²⁵ to the widths of the in-plane (110) MnF_2 Bragg reflections (after correction for instrumental broadening) yielded lower limits for twin domain sizes of 6 ± 1 and 10 ± 1 nm for samples R and S, respectively.

To confirm that the Fe overlayer is exchange coupled to the AF layer after field cooling through T_N , the F hysteresis loops of the samples (Fig. 1) were measured with a superconducting quantum interference device magnetometer. The samples were cooled to 10 K ($< T_N$) in a field of $H_{FC} = 2$ kOe ($= 159$ k A/m) with the orientation shown in Fig. 1 (inset). $H_E = -32 \pm 3$ Oe and $H_C = 138 \pm 4$ Oe for sample R, and $H_E = -30 \pm 2$ Oe and $H_C = 81 \pm 2$ Oe for sample S,²⁶ which are consistent with previous measurements on similarly grown bilayers.²¹ Above T_N , $H_C = 43 \pm 2$ Oe for sample R and 10 ± 2 Oe for sample S.

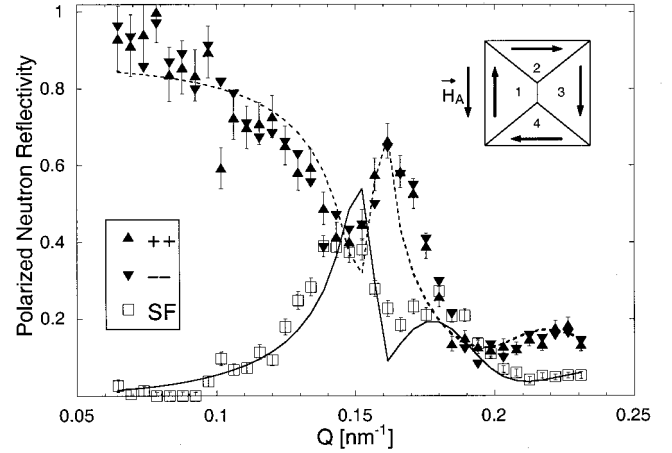


FIG. 2. Polarized neutron reflectivity of sample S corresponding to (\square) in Fig. 1 measured as a function of momentum transfer Q . The curves were obtained from a one-parameter fit of a closure domain model (inset) to the data.

The magnitude and orientation of the magnetization vector \mathbf{M} relative to the cooling field were determined from sample reflectivities measured with polarized neutrons. PNR involves specular reflection of a polarized neutron beam from a flat sample onto a polarization analyzer.²⁷ Four neutron cross sections were measured. Two cross sections correspond to the non-spin-flip (NSF) reflectivity profiles, where the intensities of the reflected radiation for spin-up ($++$) [and alternately spin-down ($--$)] neutrons illuminating and reflecting from the sample were measured. The difference between the $++$ and $--$ NSF reflectivity profiles, ΔNSF , is related to the projection of \mathbf{M} on the direction of the applied field, i.e., $\Delta\text{NSF} \propto \mathbf{M}_{\parallel}$. The remaining two cross sections are the spin-flip (SF) reflectivities. These are nonzero if the sample changes the neutron beam polarization from spin up to spin down ($+-$), and vice versa. For most neutron-scattering studies, the two SF cross sections ($+ -$ and $- +$) are equal (and this experiment is no exception),²⁸ so here the average of the $+ -$ and $- +$ cross sections is called SF. If \mathbf{M} has a component \mathbf{M}_{\perp} perpendicular to the neutron spin, then the beam polarization will change, so $\text{SF} \propto \mathbf{M}_{\perp}$. Note, the difference between the NSF cross sections is related to \mathbf{M}_{\parallel} , in contrast to the SF cross section, which is related to \mathbf{M}_{\perp} .

For the neutron-scattering experiment, the samples were cooled (to 36 K for sample S and 20 K for sample R) in a field $H_{FC} = 2.00 \pm 0.01$ kOe with the orientation shown in Fig. 1 (inset). Subsequent neutron measurements involved saturating the sample in a +2-kOe field,²⁹ reducing the applied field to zero, reversing the direction of the applied field and then increasing the field strength until the $++$ and $--$ reflectivity profiles were equal, i.e., $\Delta\text{NSF} = 0$. This field corresponds to $-H_C(T) + H_E(T)$ (\square 's in Fig. 1) where $\mathbf{M}_{\parallel} = 0$. The two NSF ($++$ and $--$) and two SF ($+ -$ and $- +$) cross sections were then measured in a region of momentum transfer Q , close to the critical edge³⁰ of the sample (Fig. 2). In all cases, the two SF cross sections were found to be equal, so the average of the two cross sections is shown in Fig. 2. If a closure domain model³¹ (Fig. 2, inset) is assumed

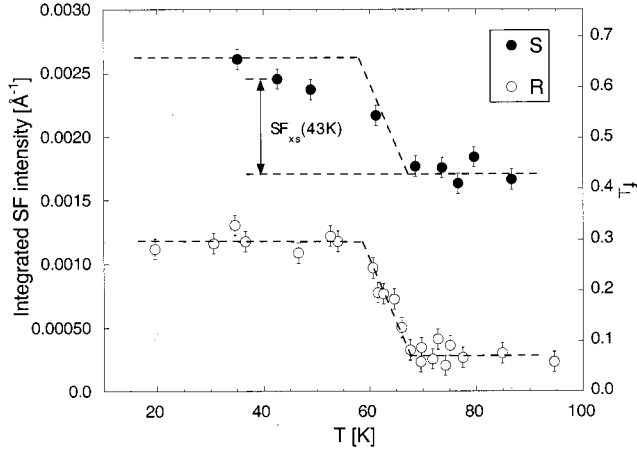


FIG. 3. Temperature dependence of the SF scattering normalized to NSF scattering (Fig. 2), integrated over Q , is shown for samples S (●) and R (○). The dashed line is a guide to the eye for the data taken from sample R. The dashed line is shifted upwards for sample S to emphasize the difference in the temperature dependencies of the SF scattering between the two samples. f_{\perp} represents the fraction of the Fe film with magnetization perpendicular to the applied field \mathbf{H}_A , i.e., $f_{\perp} = f_2 + f_4$ (see Fig. 1, inset). The spin-flip scattering in excess of that measured above T_N , SF_{xs} , is shown in the figure for one measurement.

for the Fe film domain structure at coercivity, then the SF intensity is directly proportional to $f_{\perp} = f_2 + f_4$. f_{\perp} represents the fraction of the Fe film with magnetization perpendicular to the applied field, and f_i is a scalar variable representing the fraction of the sample with magnetization corresponding to that of the i th ($i = 1, 2, 3$, or 4) domain (Fig. 2, inset). Within the formalism of the closure domain model, \mathbf{M}_{\perp} is related to $|\mathbf{M}|$ through f_{\perp} , i.e., $|\mathbf{M}_{\perp}| = f_{\perp} |\mathbf{M}|$. The curves in Fig. 2 represent the NSF and SF reflectivity profiles obtained from a closure domain model in which only f_{\perp} was optimized to achieve the best fit to the data.³² The agreement between the one-parameter fit and the data is excellent.

The measurement procedure was repeated several times in the temperature range from 20–324 K. The SF intensity integrated over the measured Q range (from 0.065–0.23 nm^{-1}) is plotted (sample S: ● sample R: ○) as a function of temperature in Fig. 3. f_{\perp} , which is related to the integrated SF intensity (by fitting to the closure domain model), is shown on the axis at the right of Fig. 3. For $T > T_N$, the integrated SF intensity (or f_{\perp}) is nonzero for both samples (Fig. 3), indicating that in the absence of exchange coupling across the F-AF interface, magnetization rotation still occurs on the upper branch of the hysteresis loop. The predominance of magnetization rotation in the smooth sample (above T_N) compared to the rough sample, and differences in H_C between the samples above T_N , stem from differences in the anisotropies of the Fe films, since they have different microstructures.

However, for $T < T_N$, both samples show a very pronounced enhancement of SF intensity (Fig. 3). This suggests that \mathbf{M}_{\perp} at coercivity increases below T_N due to AF ordering

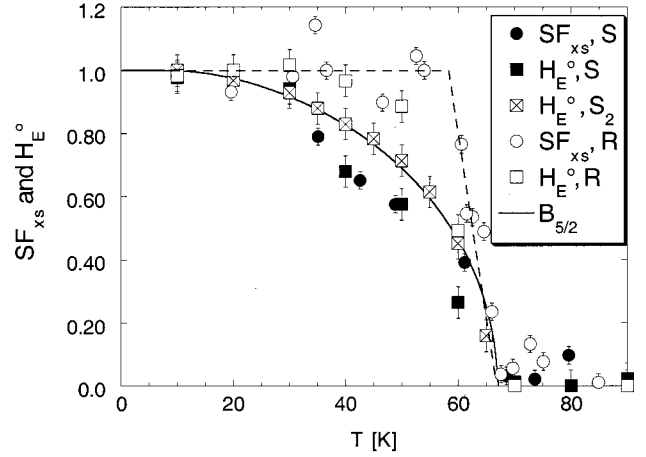


FIG. 4. Temperature dependence of H_E normalized to unity, H_E^o (boxes), is shown for the samples. The SF scattering in excess to that measured above T_N , SF_{xs} (circles), is normalized to $H_E^o(50 \text{ K})$ for the respective sample. The solid curve is the Brillouin function for a spin = $\frac{5}{2}$ system and $T_N = 67 \text{ K}$. The dashed lines are guides to the eye.

in MnF_2 and the concomitant exchange coupling across the F-AF interface. For sample S, a steady decrease of the integrated SF intensity (or f_{\perp}) is observed as T_N is approached from below. On the other hand, the integrated SF intensity from sample R shows less temperature dependence until a temperature close to T_N is reached; then the intensity decreases.

Next, we compare $H_E(T)$ to the thermal response of the F overlayer magnetization at coercivity. $H_E(T)$ normalized to $H_E(0 \text{ K})$, called $H_E^o(T)$, is plotted in Fig. 4 (boxes). $H_E^o(T)$ data are also shown for a second (smooth) sample S_2 , with interfacial roughness of $0.36 \pm 0.15 \text{ nm}$ —slightly less than that of sample S ($0.5 \pm 0.2 \text{ nm}$). The slope of H_E^o close to T_N , $-dH_E^o/dT$,³³ is shown in Fig. 5 for several Fe- MnF_2 samples (including samples R and S) with different interfacial roughness. A tendency for the rate in the drop of H_E near T_N to be correlated with interfacial roughness for many Fe- MnF_2 samples (with the notable exception of sample S_2) is observed. Specifically, the approach of H_E^o to T_N is steepest for samples with the roughest interfaces. The integrated SF intensity (or f_{\perp}) above a mean value obtained from the $SF(T > T_N)$ in Fig. 3, and normalized to H_E^o , is shown in Fig. 4 (circles) for the respective samples. This excess SF intensity is called SF_{xs} . The temperature dependencies of the neutron SF intensity (related to f_{\perp}) and the exchange bias for the smooth sample (sample S) are remarkably correlated. Specifically, the temperature dependence shows a monotonic decrease in the SF intensity (or f_{\perp}) and exchange bias for the smooth sample (sample S) with increasing temperature. A similar correlation is observed between the temperature dependencies of the SF intensity and exchange bias for the rough sample (sample R). However, in contrast to sample S, the temperature dependence reflected in the SF intensity an-exchange bias for the rough sample is constant until a temperature close to T_N , and then a precipitous decrease occurs.

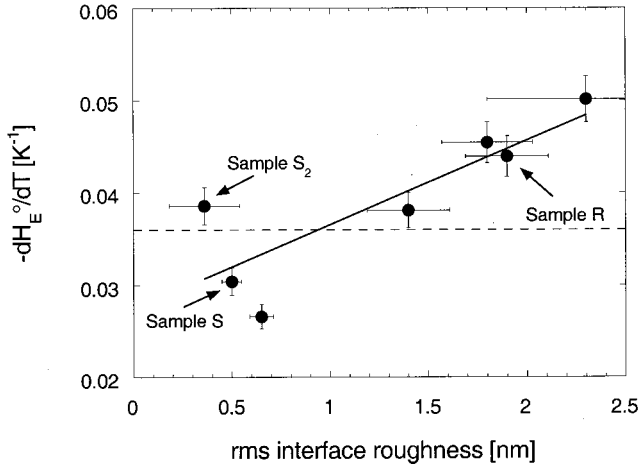


FIG. 5. The derivative of H_E^o with respect to temperature T as $T \rightarrow T_N$ is shown for several Fe-MnF₂ samples with different interface roughness. The solid line is a linear fit to the data, which suggests a tendency for $|dH_E^o/dT|$ to increase with increasing interface roughness. The dashed line, corresponding to $dH_E^o/dT = -0.036 \text{ K}^{-1}$, is the derivative of the Brillouin function (shown in Fig. 4) as $T \rightarrow T_N$.

The strong correlation between $SF_{xs}(T)$ and $H_E^o(T)$ for smooth and rough samples is remarkable, since $SF_{xs}(T)$ is obtained from an observation taken from only *one* side of the hysteresis loop, while $H_E^o(T)$ is obtained from a comparison of coercive fields from *both* sides of the loop. The implication of this correlation is that the temperature dependencies of magnetization reversal processes on either side of the loop must be the same, because $SF_{xs}(T)$ is correlated with $H_E^o(T)$ —a measurement obtained from both sides of the loop. Yet, interestingly, the reversal processes are very different. The cooling field orientation shown in Fig. 1 (inset) is one that promotes asymmetric magnetization reversal—on the left-hand side of the loop, reversal occurs via magnetization rotation (hence \mathbf{M}_\perp and SF are nonzero), while on the right-hand side reversal occurs via domain nucleation and wall motion.

Several theoretical models attributing the origin of exchange bias to the formation of AF domains^{13,14,34} predict a temperature dependence of $H_E(T) \propto \sqrt{K_1(T)}$, where K_1 is the anisotropy of bulk MnF₂. We note that for bulk MnF₂, $\sqrt{K_1}$ and the Mn²⁺ sublattice magnetization have the same temperature dependence,^{35,36} the latter having been previously measured with neutron scattering.³⁷ This work determined the temperature dependence of the sublattice magnetization to be the same as a Brillouin function for an $S = \frac{5}{2}$ system, $B_{5/2}(T)$ with $T_N = 67 \text{ K}$; therefore, the same models that predict $H_E(T) \propto \sqrt{K_1(T)}$ also predict that $H_E(T) \propto B_{5/2}(T)$. $B_{5/2}(T)$ is shown by the solid curve in Fig. 4.³⁸ We note $H_E(T)$ for the sample with the smoothest F-AF interface (sample S₂) is nearly identical to that of $B_{5/2}(T)$. For the case of the sample with a rough F-AF interface, the temperature dependence of the integrated SF intensity is not “Brillouin-like,” i.e., the integrated SF intensity and H_E show little appreciable change with temperature until just

below T_N , then decrease precipitously.

However, other models can also produce the observed $H_E(T)$ in the smoothest sample. For example, in F-AF systems that can exhibit positive exchange bias (e.g., samples S and S₂ for $H_{FC} > 20 \text{ kOe}$), the exchange coupling across the smooth Fe-MnF₂ interface is antiferromagnetic (irrespective of H_{FC}).³⁹ Leighton *et al.*²¹ and Hong⁴⁰ have attributed the origin of AF coupling across the Fe-MnF₂ interface to superexchange⁴¹ between Fe^{2+} - F^+ - Mn^{2+} . In this model, the AF coupling across the Fe-MnF₂ interface is expected to increase with decreasing temperature in proportion to the AF-sublattice magnetization (as observed for sample S₂).

In the case of the rough sample, an altogether different temperature dependence of the magnetization reversal process (and H_E) was observed. Possible origins include roughness-induced alteration of the temperature dependence of the AF surface magnetization⁴² or a difference due to fundamentally different interfacial exchange coupling.³⁹ We note that sample R is an example of a system that exhibits only negative exchange bias (for any H_{FC}), so the Fe film is ferromagnetically coupled to the MnF₂.³⁹ Leighton *et al.*²¹ attribute F-coupling across the rough Fe-MnF₂ interface to direct exchange (plus superexchange) between Fe and Mn atoms. In addition, roughness-induced uncompensated free spins at the F-AF interface could provide a contribution to H_E . We believe the strong F (direct) coupling between Fe and uncompensated Mn spins would tend to promote magnetic order of the F-AF interface at higher temperature (near T_N), since the uncompensated moments would be less constrained (via exchange) to the MnF₂ sublattice magnetization.

In summary, we measured the response (the intensity of spin-flip scattering and exchange bias) of Fe films exchange coupled to an AF (MnF₂). The temperature dependencies of the fraction of magnetization perpendicular (i.e., SF_{xs}) to the applied field at coercivity and $H_E(T)$ are remarkably well correlated. For a sample with a smooth F-AF interface, both quantities decreased monotonically with increasing temperature. In contrast, little temperature dependence was observed in the magnetization reversal process or $H_E(T)$ for a sample with an imperfect (rough or interdiffused) F-AF interface until the sample temperature was raised to within $\sim 10 \text{ K}$ of T_N . In other words, a range in dependencies of magnetic response to changing temperature was observed and is attributable to disorder of the F-AF interface. The thermal response of an F overlayer at coercivity, and consequently H_E , are fundamentally different for F-AF interfaces with different structural disorder.

The neutron-scattering facilities of the National Institute of Standards and Technology and the Hahn-Meitner Institute are gratefully appreciated. We acknowledge discussions with D. Martien. This work was supported by the U.S. Department of Energy, BES-DMS under Contract No. W-7405-Eng-36, Grant No. DE-FG03-87ER-45332, the National

Science Foundation, and funds from the University of California Collaborative University and Laboratory Assisted Research. Two of us (A.H. and P.C.Y.) thank the Los Alamos National Laboratory for its support through its director's

funded postdoctoral fellowship program. Partial funding was also received from Catalan DGR (1999SGR00340). J.N. acknowledges support from the European Union under the Human Potential Program (HPRI-1999-CT00020).

- *Present address: Department of Chemical Engineering and Materials Science, University of Minnesota, Minneapolis, MN 55455.
- ¹W. H. Meiklejohn and C. P. Bean, *Phys. Rev.* **105**, 904 (1957).
 - ²B. Dieny, V. Speriosu, S. S. P. Parkin, B. A. Gurney, D. R. Wilhoit, and D. Mauri, *Phys. Rev. B* **43**, 1297 (1991); A. E. Berkowitz and K. Takano, *J. Magn. Magn. Mater.* **200**, 552 (1999).
 - ³For a review, see J. Nogués and Ivan K. Schuller, *J. Magn. Magn. Mater.* **192**, 203 (1999).
 - ⁴J. Nogués, T. J. Moran, D. Lederman, Ivan K. Schuller, and K. V. Rao, *Phys. Rev. B* **59**, 6984 (1999); C.-M. Park, K.-I. Min, and K. H. Shin, *J. Appl. Phys.* **79**, 6228 (1996).
 - ⁵C. Leighton, J. Nogués, B. J. Jönsson-Åkerman, and Ivan K. Schuller, *Phys. Rev. Lett.* **84**, 3466 (2000).
 - ⁶J. W. Cai, Kai Liu, and C. L. Chien, *Phys. Rev. B* **60**, 72 (1999); D. V. Dimitrov, S. Zhang, J. Q. Xiao, G. C. Hadjipanayis, and C. Prados, *ibid.* **58**, 12 090 (1998).
 - ⁷The coercivity H_C is the half width of the hysteresis loop measured between points where the projection of the sample magnetization along the direction of the applied field is zero.
 - ⁸M. R. Fitzsimmons, P. Yashar, C. Leighton, Ivan K. Schuller, J. Nogués, C. F. Majkrzak, and J. A. Dura, *Phys. Rev. Lett.* **84**, 3986 (2000).
 - ⁹V. I. Nikitenko, V. S. Gornakov, A. J. Shapiro, R. D. Shull, Kai Liu, S. M. Zhou, and C. L. Chien, *Phys. Rev. Lett.* **84**, 765 (2000).
 - ¹⁰K. Takano, R. H. Kodama, A. E. Berkowitz, W. Cao, and G. Thomas, *Phys. Rev. Lett.* **79**, 1130 (1997).
 - ¹¹T. Ambrose and C. L. Chien, *J. Appl. Phys.* **83**, 6822 (1998); C. Schlenker, S. S. P. Parkin, J. C. Scott, and K. Howard, *J. Magn. Magn. Mater.* **54–57**, 801 (1986); C. Tsang and K. Lee, *J. Appl. Phys.* **53**, 2605 (1982); M. F. Toney, C. Tsang, and J. K. Howard, *ibid.* **70**, 6227 (1991).
 - ¹²R. L. Stamps, *J. Phys. D* **33**, R247 (2000).
 - ¹³D. Mauri, H. C. Siegmann, P. S. Bagus, and E. Kay, *J. Appl. Phys.* **62**, 3047 (1987).
 - ¹⁴A. P. Malozemoff, *Phys. Rev. B* **35**, 3679 (1987).
 - ¹⁵N. C. Koon, *Phys. Rev. Lett.* **78**, 4865 (1997).
 - ¹⁶M. Kiwi, J. Mejia-Lopez, R. D. Portugal, and R. Ramirez, *Appl. Phys. Lett.* **75**, 3995 (1999).
 - ¹⁷T. C. Schulthess and W. H. Butler, *Phys. Rev. Lett.* **81**, 4516 (1998).
 - ¹⁸Harry Suhl and Ivan K. Schuller, *Phys. Rev. B* **58**, 258 (1998).
 - ¹⁹T. Ambrose and C. L. Chien, *Phys. Rev. Lett.* **76**, 1743 (1996).
 - ²⁰N. B., the magnitude of H_E decreased.
 - ²¹C. Leighton, J. Nogués, Harry Suhl, and Ivan K. Schuller, *Phys. Rev. B* **60**, 12 837 (1999).
 - ²²L. G. Parratt, *Phys. Rev.* **95**, 359 (1954).
 - ²³Deviations of interface heights about a mean value (roughness) are averaged over lateral dimensions (on the order of microns), which are determined by the coherence of the x ray or neutron beam.
 - ²⁴H. Dosch, *Phys. Rev. B* **35**, 2137 (1987).
 - ²⁵B. E. Warren, *X-Ray Diffraction* (Dover, New York, 1990), p. 253.
 - ²⁶These values of H_E and H_C were measured at 20 K.
 - ²⁷G. P. Felcher, R. O. Hilleke, R. K. Crawford, J. Hanmann, R. Kleb, and G. Ostrowski, *Rev. Sci. Instrum.* **58**, 609 (1987); C. F. Majkrzak, *Physica B* **221**, 342 (1996).
 - ²⁸One exception would be a spiral spin structure with a direction of propagation parallel to the reflecting film surface.
 - ²⁹“+” and “-” refer to whether the applied field is parallel or antiparallel to the cooling field, respectively.
 - ³⁰I.e., the region in Q where the sample reflectivity is nearly 100%.
 - ³¹J. Crangle, *Solid State Magnetism* (Van Nostrand Reinhold, New York, 1991), p. 163.
 - ³²The magnitude of the net sample magnetization is needed for fitting. The magnitude was determined from fits to data taken from the samples in saturation, i.e., for $f_{\perp} = 0$, and held constant in fitting the data taken at coercivity where $f_{\perp} \neq 0$.
 - ³³To obtain the slope of $H_E(T)$ close to T_N , a third-order polynomial was fitted to the data in the range $50 < T < 67.3$ K, and the linear slope as $T \rightarrow T_N$ was extracted.
 - ³⁴P. Miltényi, M. Gierlings, J. Keller, B. Beschoten, G. Güntherodt, U. Nowak, and K. D. Usadel, *Phys. Rev. Lett.* **84**, 4224 (2000).
 - ³⁵S. Foner, *Phys. Rev.* **107**, 683 (1957).
 - ³⁶U. Gäfvert, L. Lundgren, P. Nordbald, B. Westerstrandh, and O. Beckman, *Solid State Commun.* **23**, 9 (1977).
 - ³⁷R. A. Erickson, *Phys. Rev.* **90**, 779 (1953).
 - ³⁸J. Crangle, *Solid State Magnetism* (Van Nostrand Reinhold, New York, 1991), p. 109.
 - ³⁹J. Nogués, C. Leighton, and Ivan K. Schuller, *Phys. Rev. B* **61**, 1315 (2000).
 - ⁴⁰T. M. Hong, *Phys. Rev. B* **58**, 97 (1998).
 - ⁴¹P. W. Anderson, *Phys. Rev.* **115**, 2 (1959).
 - ⁴²D. Lederman, J. Nogués, and Ivan K. Schuller, *Phys. Rev. B* **56**, 2332 (1997).